Rational fabrication of chitosan/alginate/silica ternary aerogel beads adsorbent with free separation

Wei Wei[1,2] ✉, *Huihui Hu*[2], *Sijia Yin*[3], *Yanxiao Li*[1], *Xuelin Ji*[1], *Jimin Xie*[2]

[1]*Center of Analysis and Test, Jiangsu University, Zhenjiang, 212013, People's Republic of China*
[2]*School of Chemistry and Chemical Engineering, Jiangsu University, Zhenjiang, 212013, People's Republic of China*
[3]*School of Food and Biological Engineering, Jiangsu University, Zhenjiang 212013, People's Republic of China*
✉ *E-mail: weiwei@ujs.edu.cn*

Published in Micro & Nano Letters; Received on 15th July 2018; Revised on 3rd September 2018; Accepted on 1st October 2018

Novel chitosan/alginate/silica ternary aerogel beads were successfully prepared by the orifice-coagulation bath with the ambient pressure drying method and utilising chitosan, sodium alginate, and tetraethoxysilane as the initial raw materials. The morphologies, porosity characteristics, and dye absorbencies of the ternary aerogel beads were also investigated, respectively. The obtained samples are milky light solid, the size of the spherical aerogel is uniform, its diameter can be controlled ~5 mm, the specific surface area is 169.4 m^2 g^{-1}, pore size distribution is concentrated in the 2–100 nm, which is a typical nanofilamentous network structure. Meanwhile, the ternary beads were tested for dyestuffs adsorption; the results showed that the obtained samples exhibit excellent adsorption properties, and can keep good sphericity as a class of novel adsorbents.

1. Introduction: Silica aerogels as unique porous materials are being used in both scientific and commercial applications because of high porosity, high specific surface area, large pore volumes, low density, and low-thermal conductivity [1–4]. With the development of aerogels preparation technology, synthesising silica hybrid aerogels with special and improved properties have been considered as a rational process to expand the broad range of applications of aerogels [5–7]. Mazraeh-Shahi *et al.* improved the flexibility of silica aerogels using hydrogen-bonding links between polyurethane and silica causing polyurethane chains to be preserved as a part of the gel network [5]. Wang *et al.* synthesised chitosan–silica composite aerogels adsorbent successfully. The Congo red adsorption onto this adsorbent reaches as high as about 150 mg/g [6]. Ulker *et al.* developed a silica hybrid aerogels consisting of a silica aerogel core encapsulated by an alginate aerogel layer [7]. The authors claimed that hybrid aerogels have advantages to tailor their structural properties according to specific requirements.

However, research on silica hybrid aerogels has been mainly focused on monolithic aerogels. Nowadays, reports on silica hybrid aerogels beads are attracted more attention in adsorption study. Zhai *et al.* prepared cellulose-based aerogel microspheres that demonstrated an ultrahigh crude oil absorption capacity [8]. Zhang *et al.* reported a facile method for synthesising poly(sodium acrylate)-modified tetramethyl-1-piperidinyloxy-oxidised cellulose nanofibril aerogel spheres. The water absorbent capacity of the aerogel spheres could be as high as 1030 g/g [9]. Meanwhile, aerogel beads offer additional desirable features, such as controllable particle sizes and pore structures, which will be developed to meet a variety of industrial wastewater treatment demands.

In this work, we report the synthesis of crack-free chitosan/alginate/silica ternary aerogel beads adsorbent with free separation and high polysaccharide content by the orifice-coagulation bath (OCB). The inhomogeneity has been prevented by preparing single polysaccharide beads sols firstly and mixing them to get hybrid sols individually. The method has been effectively simplified. The structural properties of the ternary aerogel beads have been investigated comparing with binary aerogel beads. In addition, the morphologies, porosity characteristics, physical properties, and absorbencies of the ternary aerogel beads were systematically studied.

2. Experimental

2.1. Materials: Tetraethoxysilane (TEOS), chitosan (deacetylation degree >95%), acetic acid, calcium chloride ($CaCl_2$), sodium alginate, *n*-hexane, and ethanol are all analytically pure and purchased from Sinopharm Chemical Reagent Co. Ltd, China.

2.2. Synthesis of chitosan/alginate/silica ternary aerogel beads (CTS–SA–SiO_2): Fig. 1 shows the experimental procedures used for the preparation of chitosan/alginate/silica ternary aerogel beads at ambient pressure. An aqueous solution of chitosan was obtained by dissolving chitosan (2 g) and $CaCl_2$ (3 g) in a solution of acetic acid (100 ml, 0.1 mol/l), which corresponded to a stoichiometric amount of acid with respect to the amount of NH_2 functions [10]. Total dissolution was obtained under stirring over 12 h at room temperature. This solution was dropped into a sodium alginate solution (2 g sodium alginate was dissolved in 100 ml deionised water under stirring overnight) through a 0.7 mm gauge syringe needle to provide gelified chitosan/alginate beads. These beads were stored in the solution for 3 h and then washed with distilled water. The chitosan/alginate beads were transferred into the beaker and washed with distilled water at 30°C for four times (each 2 h) to remove the sodium ions trapped inside the wet beads. Subsequently, the beads were immersed in ethanol at 30°C for four times (each 2 h) to remove the water remaining in their pores. After washing, the chitosan/alginate beads were immersed in ethanol/TEOS/water ($V_{ethanol}$:$V_{tetraethoxysilane}$:V_{water} = 11: 8:1) solution at 60°C for 72 h. After silica skeleton improvement, the beads were washed with *n*-hexane at 30°C for 12 h to move the unreacted TEOS. The *n*-hexane solution was refreshed every 3 h. Finally, the wet beads were dried at room temperature (~25°C) for 24 h.

2.3. Synthesis of alginate/silica binary aerogel beads (SA–SiO_2): For comparison, an aqueous solution of alginate was obtained by dissolving alginate (2 g) in deionised water (100 ml) under stirring over 12 h at room temperature. Then this solution was dropped into a calcium chloride solution (2 g $CaCl_2$ was dissolved in 150 ml deionised water) through a 0.7 mm gauge syringe needle to provide gelified alginate beads. The alginate beads were washed with distilled water at 30°C for four times (each 2 h). Then the beads were immersed in ethanol for further gelation and aging at

doi: 10.1049/mnl.2018.5394

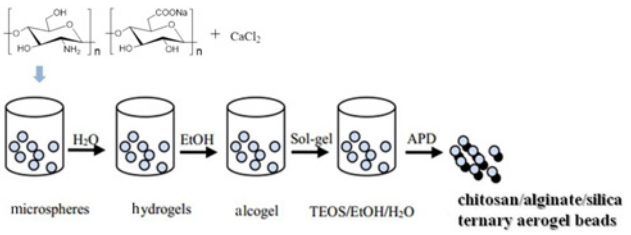

Fig. 1 *Preparation process of chitosan/alginate/silica ternary aerogel beads*

30°C for four times (each 2 h). After washing, the alginate beads were immersed in ethanol/TEOS/water solution ($V_{ethanol}$: $V_{tetraethoxysilane}$:V_{water} = 11: 8 :1) at 60°C for 72 h. Then the beads were washed with *n*-hexane at 30°C for 12 h and then *n*-hexane was refreshed every 3 h. Finally, the wet beads were dried at room temperature for 24 h.

2.4. Structural characterisation of the samples: The small angle X-ray scattering (SAXS) patterns of samples were characterised using Cu–Kα incident radiation by a Bruker-AXS D8 Advance diffractometer (50 kV, 60 mA, the range of 0.5–10°). Fourier transform infrared (FTIR) spectroscopy was performed by using a Nicolet NEXUS470 FTIR spectrometer (Thermo Scientific, USA). The Brunauer–Emmett–Teller (BET) specific surface area was obtained from the N_2 adsorption/desorption analyses at 77 K (NOVA 2000, Quantachrome). The microstructure of the aerogel beads was probed by field emission scanning electron microscopy (SEM, Model Philips XL-30SEM analyser) and transmission electron microscopy (TEM, JEOL-JEM-2010, Japan). The tapping densities and oil absorption capacity of the aerogel beads were also investigated as reported previously [11].

3. Results and discussion: Herein, Fig. 2 shows that binary (Fig. 2*a*) and ternary (Fig. 2*b*) aerogel beads prepared by OCB. In contrast, after chitosan addition, the formability of aerogel beads is slightly improved. The experimental results on the packing bed density, shape and the appearance of both aerogel beads are given in Table 1. The packing bed density study suggests chitosan content boost little density of the aerogel beads appreciably. Meanwhile, the sample SA–SiO_2 showed smaller shape than ternary aerogel beads. This is because of the fact that the chitosan–alginate complex gels keep sphericity due to the interaction of anionic alginate with the cationic chitosan, giving a cross-linking thin skin layer [12]. The SAXS was employed to confirm the mesoporous structure. As can be seen from Fig. 3, the SA–SiO_2 contains a diffraction maxima at $2\theta = 1.4°$, which can be assigned to well-ordered mesoporous structures with straight channels (Fig. 3*a*) [13]. However, there is a concave curve observed

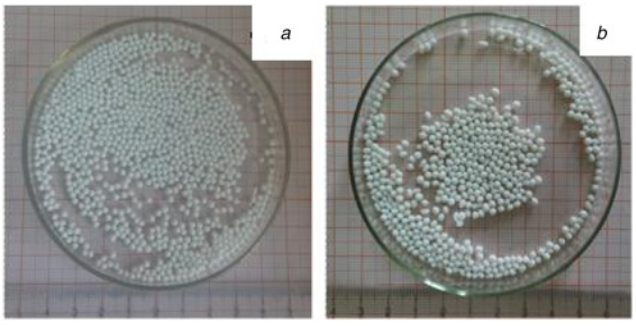

Fig. 2 *Photographs of beads*
a SA–SiO_2 and
b CTS–SA–SiO_2

Table 1 Physical properties of aerogel beads by OCB

Physical property	SA–SiO_2	CTS–SA–SiO_2
packing bed density, g/cm^3	0.155	0.160
porosity, %	91.67	90.44
oil absorption, ml/g	2.91	3.45
water absorption, ml/g	2.78	2.88
shape and appearance	spheroid milk white	spheroid milk white
BET surface area, m^2/g	160.8	169.4
pore volume, cm^3/g	0.542	0.658
average pore diameter, nm	6.598	4.940
RhB removal, %	24.56	57.45
MB removal, %	22.61	63.69

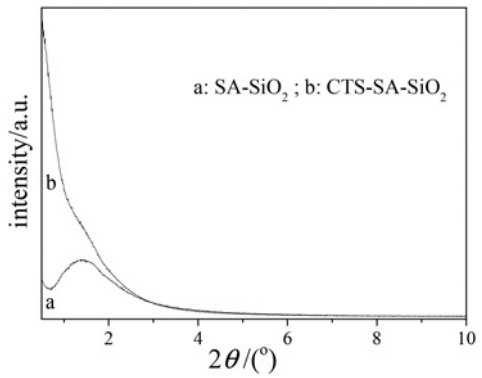

Fig. 3 *SAXS pattern of aerogel beads*
a SA–SiO_2
b CTS–SA–SiO_2

in Fig. 3*b* (CTS–SA–SiO_2). It might be lead to the heterogeneity or disorder of the mesoporous when chitosan was added.

FTIR spectroscopy was performed to confirm the function group of aerogel beads. Fig. 4 shows the FTIR spectra of SA–SiO_2 and CTS–SA–SiO_2. For both composite aerogel beads, characteristic absorptions at 1073 cm^{-1} are attributed to the stretching vibration of Si–O–Si, near 800 cm^{-1} corresponds to bending vibration of Si–O. While, the peak at about 1618 and 1400 cm^{-1} is C=O symmetric stretching vibration from the chitosan or alginate is seen in all the aerogel beads [6, 13]. In addition, the broad peak between 3150 and 3500 cm^{-1} appeared in the ternary aerogel is related to hydrogen bonds involving –NH_2 and/or –OH groups for CTS–SA–SiO_2, indicating the chitosan-base amine functionality. While for CTS–SA–SiO_2 at this region becomes broader than SA–SiO_2 due to the interaction between the carbonyl group of

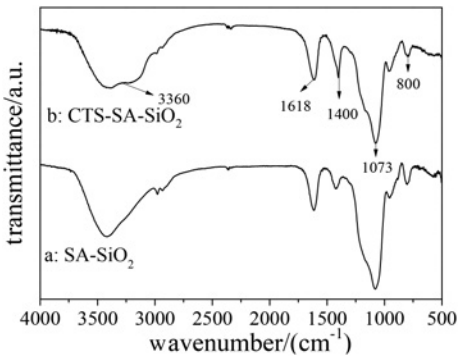

Fig. 4 *FTIR pattern of aerogel beads*
a SA–SiO_2 and
b CTS–SA–SiO_2

chitosan and the silica network occurs [14]. It can be seen that this ternary aerogel beads can be successfully prepared by incorporating chitosan cross-linked with alginate.

To study the structure morphology of aerogel beads more directly, SEM and TEM measurements were taken, and the photographs are shown in Fig. 5. We observed that the surface of both aerogel beads is coarse. Meanwhile, SA–SO_2 exhibits a porous structure while CTS–SA–SiO_2 has a micron-sized porous structure and also exhibited a looser microstructure of the internal network. The phenomenon is corresponding to the X-ray diffraction analysis. SA–SiO_2 has a honeycomb-like network structure whose sizes are at the nano level (Fig. 5*c*). Also, the pore size of SA–SiO_2 is smaller than that of CTS–SA–SiO_2. For CTS–SA–SiO_2, the fibres in the internal network are separated by void spaces >50 nm (Fig. 5*d*), thus displaying the macroporous network of the adsorbent materials. These give the evidence for the formation of a fibrous network characteristic of polysaccharide gelling polymers [10].

Fig. 6 shows the nitrogen adsorption/desorption isotherms of both aerogel beads. For both aerogel beads, the N_2 adsorption/desorption isotherms displayed the intermediate between type II and IV curves, indicating the presence of large mesopores with a size distribution which continues into the macropore domain [15]. The hysteresis loops at $P/P_0 > 0.5$ indicate the existence of slit-shaped pores and also the presence of mesopores in both aerogel beads [5]. The specific surface areas and pore volumes of the respective samples are also listed in Table 1. The meso- and macrostructures allow the rapid diffusion for adsorption [5, 16]. In conclusion, most of the previous results demonstrated that the aerogel beads exhibited excellent adsorption performance.

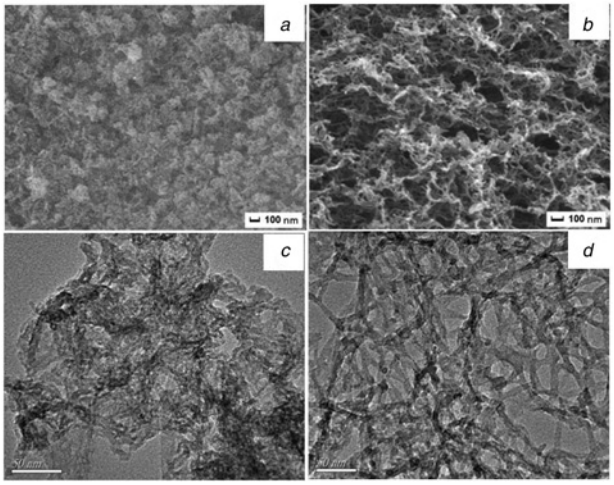

Fig. 5 *SEM and TEM photographs of aerogel beads*
a, *c* SA–SiO_2
b, *d* CTS–SA–SiO_2

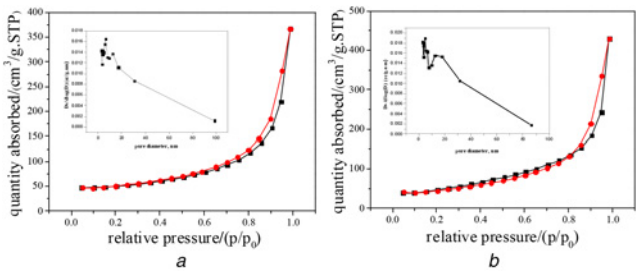

Fig. 6 *N_2 adsorption/desorption isotherms and pore size distributions (inset) of aerogel beads*
a SA–SiO_2
b CTS–SA–SiO_2

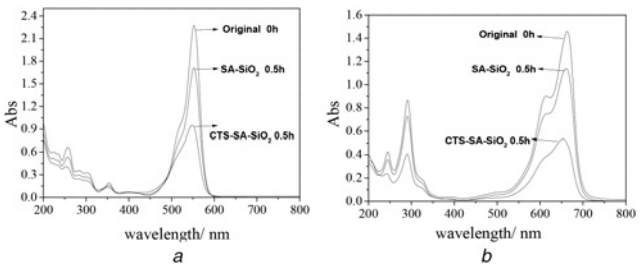

Fig. 7 *Ultraviolet–visible spectrum of adsorption of*
a RhB by two beads in 0.5 h
b MB by two beads in 0.5 h

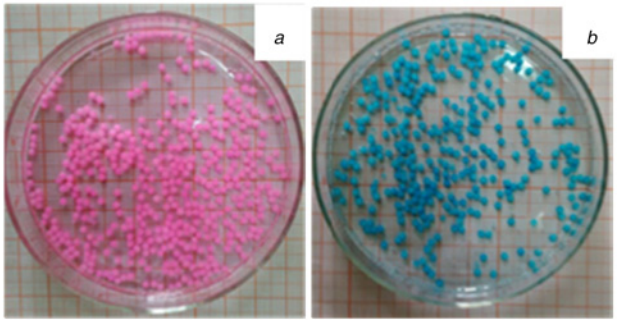

Fig. 8 *Test for absorbing ability of CTS–SA–SiO_2*
a Absorbed RhB
b Absorbed MB

The absorption capacities of the aerogel beads for different dyestuffs were measured. Two common dyestuffs, namely, rhodamine B (RhB), and methylene blue (MB) were used in Fig. 7. Also, during the same time, the dyestuffs removal (%) of the CTS–SA–SiO_2 is higher than SA–SiO_2 (see details in Table 1), which indicates that CTS–SA–SiO_2 has good application prospect in water treatment. Besides, CTS–SA–SiO_2 also has a spherical shape and had no crack on the surface of the beads no matter before or after adsorption (Fig. 8). Furthermore, repeated recycle tests were performed for CTS–SA–SiO_2 through solvent decoration [11, 17]. After the ternary aerogel beads were washed by ethanol to release the dye. This sorption separation process was repeated five times, indicating a stable sorption and recycling performance of CTS–SA–SiO_2.

4. Conclusion: In summary, chitosan/alginate/silica ternary aerogel beads adsorbents were successfully prepared and applied in adsorption of dyestuffs for the first time. Compared with alginate/silica binary aerogel beads, the modified ternary aerogel beads exhibited more macroporous network structure and excellent adsorption activity. Especially, the structural and physical properties of aerogel beads showed an interesting dependence on chitosan composition. This work opens the way to a range of important applications of ternary aerogel bead materials and provides a kind of new adsorbent material for absorbing dyestuffs with free separation.

5. Acknowledgments: This work was supported by the National Natural Science Foundation of China (grant no. 21607063) and the China Postdoctoral Science Foundation (grant no. 2018M630530).

6 References

[1] García O., Sastre R., Agua D., *ET AL.*: 'Efficient optical materials based on fluorinated-polymeric silica aerogels', *Chem. Phys. Lett.*, 2006, **427**, pp. 375–378
[2] Zu G., Shen J., Zou L., *ET AL.*: 'Nanoengineering super heat-resistant, strong alumina aerogels', *Chem. Mater.*, 2013, **25**, pp. 4757–4764

doi: 10.1049/mnl.2018.5394

[3] Gonçalves W., Morthomas J., Chantrenne P., *ET AL.*: 'Elasticity and strength of silica aerogels: A molecular dynamics study on large volumes', *Acta Mater.*, 2018, **145**, pp. 165–174
[4] Han H., Wei W., Jiang Z., *ET AL.*: 'Removal of cationic dyes from aqueous solution by adsorption onto hydrophobic/hydrophilic silica aerogel', *Colloid Surf. A*, 2016, **509**, pp. 539–549
[5] Mazraeh-Shahi Z.T., Shoushtari A.M., Bahramian A.R., *ET AL.*: 'Synthesis, pore structure and properties of polyurethane/silica hybrid aerogels dried at ambient pressure', *J. Ind. Eng. Chem.*, 2015, **21**, pp. 797–804
[6] Wang J., Zhou Q., Song D., *ET AL.*: 'Chitosan–silica composite aerogels: preparation, characterization and Congo red adsorption', *J. Sol-Gel Sci. Technol.*, 2015, **76**, pp. 501–509
[7] Ulker Z., Erkey C.: 'A novel hybrid material: an inorganic silica aerogel core encapsulated with a tunable organic alginate aerogel layer', *RSC Adv.*, 2014, **4**, pp. 62362–62366
[8] Zhai T., Zheng Q., Cai Z., *ET AL.*: 'Synthesis of polyvinyl alcohol/cellulose nanofibril hybrid aerogel microspheres and their use as oil/solvent superabsorbents', *Carbohydr. Polym.*, 2016, **148**, pp. 300–308
[9] Zhang F., Ren H., Tong G., *ET AL.*: 'Ultra-lightweight poly (sodium acrylate) modified TEMPO-oxidized cellulose nanofibril aerogel spheres and their superabsorbent properties', *Cellulose*, 2016, **23**, pp. 3665–3676
[10] Kadib A.El., Primo A., Molvinger K., *ET AL.*: 'Nanosized vanadium, tungsten and molybdenum oxide clusters grown in porous chitosan microspheres as promising hybrid materials for selective alcohol oxidation', *Chem. Eur. J.*, 2011, **17**, pp. 7940–7946
[11] Zong S., Wei W., Jiang Z., *ET AL.*: 'Characterization and comparison of uniform hydrophilic/hydrophobic transparent silica aerogel beads: skeleton strength and surface modification', *RSC Adv.*, 2015, **5**, pp. 55579–55587
[12] Mi F.L., Sung H.W., Shyu S.S.: 'Drug release from chitosan–alginate complex beads reinforced by a naturally occurring cross-linking agent', *Carbohydr. Polym.*, 2002, **48**, pp. 61–72
[13] Zhang Y., Wang X., Su Y., *ET AL.*: 'A doxorubicin delivery system: samarium/mesoporous bioactive glass/alginate composite microspheres', *Mater. Sci. Eng. C, Mater.*, 2016, **67**, pp. 205–213
[14] Al-Sagheer F., Muslim S.: 'Thermal and mechanical properties of chitosan/SiO_2 hybrid composites', *J. Nanomater.*, 2010, **2010**, pp. 1–7, doi:10.1155/2010/490679
[15] Kadib A. El., Molvinger K., Cacciaguerra T., *ET AL.*: 'Chitosan templated synthesis of porous metal oxide microspheres with filamentary nanostructures', *Microp. Mesop. Mater.*, 2011, **142**, pp. 301–307
[16] Ma Q., Liu Y., Dong Z., *ET AL.*: 'Hydrophobic and nanoporous chitosan–silica composite aerogels for oil absorption', *J. Appl. Polym. Sci.*, 2015, **132**, p. 41770
[17] Lv X., Zhao M., Chen Z., *ET AL.*: 'Prepare porous silica nanospheres for water sustainability: high efficient and recyclable adsorbent for cationic organic dyes', *Colloid Polym. Sci.*, 2018, **296**, pp. 59–70